SUBCRITICAL INSTABILITIES IN PLANE COUETTE FLOW OF VISCO-ELASTIC FLUIDS

Alexander N. Morozov and Wim van Saarloos
Instituut-Lorentz for Theoretical Physics, LION, Leiden University,
Postbus 9506, 2300 RA Leiden, The Netherlands

Abstract A non-linear stability analysis of plane Couette flow of the Upper-Convected Maxwell model is performed. The amplitude equation describing time-evolution of a finite-size perturbation is derived. It is shown that above the critical Weissenberg number, a perturbation in the form of an eigenfunction of the linearized equations of motion becomes subcritically unstable, and the threshold value for the amplitude of the perturbation decreases as the Weissenberg number increases.

Keywords: Visco-elastic flows, subcritical instabilities, amplitude equation

Introduction

In the last decades, stability of flows of polymers, emulsions, colloids etc. has attracted wide attention when it was discovered that such flows can exhibit hydrodynamic instabilities and even become turbulent at very small Reynolds numbers (Larson et al., 1990, McKinley et al., 1991, Groisman and Steinberg, 2000, Groisman and Steinberg, 2004). Unlike Newtonian turbulence, where inertia plays a destabilizing role, this *elastic turbulence* or *turbulence without inertia* (Larson, 2000) has its origin in the visco-elastic properties of the fluid. It has become a challenge to find the mechanism of the elastic instabilities and transition to turbulence.

The non-Newtonian behaviour of complex fluids originates from the interaction between the flow and the internal structure of the fluid. In water, for example, external flows do not typically disturb molecular motion since the molecular and flow velocity- and time-scales are well separated, while in complex flows polymers get stretched, emulsion and colloidal clusters get deformed and break, vesicles change their shapes etc. Since these interactions are partly reversible (e.g. the polymers return to their equilibrium conformation releasing accumulated stress) and depend on the deformation history, the fluid acquires memory and becomes visco-elastic. Naturally, this is reflected in

the equations of motion for complex fluids: the Navier-Stokes equation (written in dimensionless units)

$$Re\left[\frac{\partial \mathbf{v}}{\partial t}+(\mathbf{v}\cdot\nabla)\,\mathbf{v}\right]=-\nabla p-\nabla\cdot\boldsymbol{\tau}$$

is supplemented by a *constitutive equation* – a relation between the stress tensor $\boldsymbol{\tau}$ and the velocity-gradient tensor $(\nabla\mathbf{v})$, which is no longer a linear Newtonian equation

$$\boldsymbol{\tau}=-\left[(\nabla\mathbf{v})+(\nabla\mathbf{v})^{\dagger}\right],$$

but usually is a non-linear PDE in space and time[1]; the dagger † denotes the transposed matrix.

The main difference between Newtonian and visco-elastic equations of motion is the presence of additional non-linearity in the constitutive equation. The inertial non-linearity $Re\,(\mathbf{v}\cdot\nabla)\,\mathbf{v}$, which is responsible for instabilities and turbulence in Newtonian liquids, is of small significance for visco-elastic fluids (especially for dense polymer solutions and melts) since their large viscosity results in small Reynolds numbers $Re\sim 10^{-4}-10^{1}$. Therefore, the non-linear behaviour of the equations of motion is dominated by the elastic non-linearity, the strength of which is controlled by a dimensionless Weissenberg number $Wi=\dot{\gamma}\lambda$, where $\dot{\gamma}$ is the typical shear rate, and λ is the relaxation time of the fluid. When the Weissenberg number becomes comparable to unity, this non-linearity gives rise to non-trivial rheological phenomena: shear-rate dependent shear viscosity, and the normal-stress effect: in plane shear $v_x=\dot{\gamma}y$, the normal-stress difference $\tau_{yy}-\tau_{xx}$ is not zero as for Newtonian fluids, but grows as $\dot{\gamma}^2$ for small Wi. At larger Weissenberg numbers, the elastic non-linearity causes hydrodynamic instabilities and, possibly, transition to turbulence.

The mechanism of linear elastic instability was identified for flows with curved stream-lines (Larson et al., 1990, Joo and Shaqfeh, 1992). One of the classical examples of such a flow is realized in Taylor-Couette cell where fluid fills the gap between two coaxial cylinders made to rotate with respect to each other. In the laminar state, the fluid moves around the cylinder axis and the elastic or *hoop* stresses act on polymer molecules stretching them along the circular stream-lines and exerting extra pressure towards the inner cylinder in consequence of the normal-stress effect. When these stresses overcome viscous friction, the laminar state becomes linearly unstable – any infinitesimal

[1]Unfortunately, there is no unique constitutive equation for all visco-elastic systems and one has to choose between various standard models (Upper-Convected Maxwell model, Oldroyd-B, FENE-P etc.) (Bird et al., 1987). This choice is usually guided by two requirements: a) the model should (approximately) reproduce rheological properties of the visco-elastic system in question, b) the model should be relatively simple to allow analytical or numerical analysis.

perturbation will push a polymer from the circular stream-lines and create a secondary flow in the form of Taylor vortices. Pakdel and McKinley generalized this mechanism to arbitrary flows (Pakdel and McKinley, 1996) and proposed that there exists a universal relation between the properties of the fluid and the flow geometry which determines the conditions of the linear instability. They argued that the critical Weissenberg number is related to the characteristic curvature of the flow stream-lines and that the linear instability disappears when the curvature goes to zero. The known results on the visco-elastic instabilities in Taylor-Couette (Larson et al., 1990), cone-and-plate and parallel plate (McKinley et al., 1991), Dean and Taylor-Dean (Joo and Shaqfeh, 1992) flows are in agreement with this *curved stream-lines – linear instability* paradigm.

The situation is different for visco-elastic parallel shear flows. There is no general agreement on whether flows like plane Couette or pipe flow do in fact become unstable. The only results available are on the linear stability of these flows. For essentially all studied visco-elastic models, laminar plane Couette flow is linearly stable (Gorodtsov and Leonov, 1967, Renardy and Renardy, 1986, Renardy, 1992, Wilson et al., 1999) (note the exception (Grillet et al., 2002)). In the case of pipe flow, the linear stability was demonstrated numerically by Ho and Denn (Ho and Denn, 1978) for any value of the Weissenberg and Reynolds numbers. Therefore, it has become common knowledge that the parallel shear flows of fluids obeying simple visco-elastic models (UCM, Oldroyd-B, etc.) are linearly stable, in agreement with the *curved stream-lines – linear instability* paradigm. Clearly, if an instability does occur in practice, it has to be non-linear.

At the moment, there has been no experiment that would clearly establish the presence or absence of a bulk hydrodynamic instability in parallel visco-elastic shear flows. One of a few indirect indications that a bulk instability might occur in pipe flow comes from the famous melt-fracture problem (Petrie and Denn, 1976, Denn, 1990, Denn, 2001), which arises in extrusion of a dense polymer solution or melt through a thin capillary. There, when the extrusion rate exceeds some critical value, the surface of the extrudate becomes distorted and the extrudate might even break, giving the name to the phenomenon. It is possible that this is a manifestation of an instability taking place inside the capillary, though other mechanisms (such as stick-slip, influence of the inlet, etc.) have been proposed (Petrie and Denn, 1976, Denn, 1990, Denn, 2001). Recently, we presented arguments for the bulk instability being related to the melt-fracture phenomenon (Meulenbroek et al., 2003, Bertola et al., 2003, Meulenbroek et al., 2004), but the issue stays controversial. There is also some evidence for non-linear parallel shear flow instabilities from numerical simulations of visco-elastic hydrodynamic equations (Atalik and Keunings, 2002). Partly because the numerical schemes used to solve these equations are

known to break down when elastic stresses become large ($Wi \gtrsim 1$) – the so-called *high Weissenberg number problem* (Owens and Phillips, 2002) – it is open to debate whether an observed phenomenon is due to a numerical or a true physical instability.

In this paper we argue that visco-elastic plane Couette flow does exhibit a subcritical instability as can be seen from the following argument. The laminar velocity profiles of the parallel shear flows have straight stream-lines, and, therefore, their linear stability is in agreement with the *curved stream-lines – linear instability* paradigm. The linear theory predicts that a small perturbation superimposed on top of the laminar flow will decay in time with the decay rate depending on the Weissenberg number. When Wi becomes larger than one, the decay time becomes comparable with the elastic relaxation time λ, and the perturbation becomes long-living. Thus, on short time-scales, the superposition of the laminar flow and the slowly-decaying perturbation can be viewed as a new basis profile *with* curved stream-lines. Applying the same *curved stream-lines – linear instability* paradigm to the perturbed streamlines, we conclude that this new flow can become linearly unstable. The instability requires a subsequent creation of two perturbations, and thus is non-linear. Since the initial perturbation has to be strong enough to become unstable, there exists a finite-amplitude threshold for the transition, which becomes smaller as the Weissenberg number increases. This scenario resembles transition to turbulence in parallel shear flows of Newtonian fluids. There as well, one encounters the absence of the linear instability, and a subcritical transition with the threshold going down with the Reynolds number (Schmid and Henningson, 2001, Hof et al., 2003).

In order to check our hypothesis we perform the non-linear stability analysis of the Upper-Convected Maxwell (UCM) model. The method we employ is somewhat similar to what was used by Stuart (Stuart, 1960) and Herbert (Herbert, 1980) for Newtonian flows. We start from the laminar plane Couette flow and perturb it by a finite-size disturbance chosen to be in the form of an eigenmode of the linear part of the equations of motion. We then derive an amplitude equation that determines the time evolution of the disturbance. The instability is found for given eigenmode, if there is such an initial value of the amplitude of the disturbance that it will grow in time and, possibly, saturate. In the following Sections we present the derivation and main results of our analysis.

1. Asymptotic expansion

Let us consider plane Couette flow of a visco-elastic fluid. The fluid is confined in-between two plates a distance $2d$ apart moving with equal velocities v_0 in the opposite directions. We use the standard convention for the coordinates with x, y, and z referring to the streamwise, gradient, and spanwise directions,

respectively. We define the Weissenberg $Wi = \lambda v_0/d$ and the Reynolds numbers $Re = \rho v_0 d/\eta$, where ρ is the density and η is the viscosity of the fluid; d is used as the unit of length, d/v_0 as the unit of time, and the stress tensor is scaled with $\eta v_0/d$.

The equations of motion include the Navier-Stokes equation

$$Re\left[\frac{\partial \mathbf{v}}{\partial t} + (\mathbf{v}\cdot\nabla)\,\mathbf{v}\right] = -\nabla p - \nabla\cdot\boldsymbol{\tau}, \tag{1}$$

and the incompressibility condition

$$\nabla\cdot\mathbf{v} = 0, \tag{2}$$

where p is the pressure, and $\boldsymbol{\tau}$ is the visco-elastic stress tensor. To close this system of equations one needs to specify the constitutive relation, and in this work we are going to use the Upper-Convected Maxwell (UCM) model

$$\boldsymbol{\tau} + Wi\left[\frac{\partial \boldsymbol{\tau}}{\partial t} + \mathbf{v}\cdot\nabla\boldsymbol{\tau} - (\nabla\mathbf{v})^{\dagger}\cdot\boldsymbol{\tau} - \boldsymbol{\tau}\cdot(\nabla\mathbf{v})\right] = -\left[(\nabla\mathbf{v}) + (\nabla\mathbf{v})^{\dagger}\right] \tag{3}$$

– one of the simplest non-linear models available. Although it does not reproduce realistic features of dense polymer solutions (Bird et al., 1987), it does predict the normal-stress effect, which is, as we have argued above, at the origin of the non-linear instabilities in parallel shear flows of visco-elastic fluids. Since our purpose is to demonstrate that such an instability *can* occur, this simple model will suffice.

As usually, we split the hydrodynamic fields $\mathbf{v}$ and $\boldsymbol{\tau}$ in two parts – the laminar value and the perturbation field:

$$\begin{aligned}
&\mathbf{v} = y\,\mathbf{e}_x + \mathbf{v}',\\
&\tau_{ij} = -2\,Wi\;\delta_{ix}\delta_{jx} - (\delta_{ix}\delta_{jy} + \delta_{iy}\delta_{jx}) + \tau'_{ij}.
\end{aligned}$$

Next, we introduce the perturbation vector $V = \{v'_i, \tau'_{ij}, p\}^{\dagger}$ and rewrite the system (1)-(3) in the compact form

$$\hat{\mathcal{L}}\,V + \hat{A}\frac{\partial V}{\partial t} = N\,(V, V)\,, \tag{4}$$

where $\hat{\mathcal{L}}$ and N represent the linear operator and the quadratic non-linearity in (1)-(3), and $\hat{A}$ is a constant diagonal matrix. The explicit expressions for $\hat{\mathcal{L}}$, N and $\hat{A}$ are given in Appendix.

Our stability analysis of eq.(4) is based on the eigenfunctions $V_0^{(n)}$ of the linear operator $\hat{\mathcal{L}}$:

$$\hat{\mathcal{L}}\left(e^{i(k_x x + k_z z)}V_0^{(n)}(y)\right) = -\lambda_n e^{i(k_x x + k_z z)}V_0^{(n)}(y). \tag{5}$$

The minus sign in the definition of the eigenvalues λ_n is chosen in such a way that $e^{\lambda_n t}e^{i(k_x x+k_z z)}V_0^{(n)}(y)$ is a solution of the linear problem $\left(\hat{\mathcal{L}}+\hat{A}\frac{\partial}{\partial t}\right)V=0$. There are several kinds of eigenfunctions of the UCM plane Couette flow and their form and number will be discussed in Section 2. Here, we will focus on a particular eigenfunction $e^{i(k_x x+k_z z)}V_0(y)$ and assume that the non-linear dynamics of eq.(4) is dominated by V_0. Then, the solution to eq.(4) can be approximated by

$$\begin{aligned} V(\mathbf{r},t) &= \Phi(t)e^{i(k_x x+k_z z)}V_0(y)+\Phi^*(t)e^{-i(k_x x+k_z z)}V_0^*(y) \\ &+U_0(y,t)+\sum_{n=2}^{\infty}\left[U_n(y,t)e^{in(k_x x+k_z z)}+U_n^*(y,t)e^{-in(k_x x+k_z z)}\right], \end{aligned} \tag{6}$$

where we have introduced the time-dependent amplitude $\Phi(t)$; * denotes complex conjugation. Moreover, we notice that the higher order harmonics U_n can only be generated by at least n non-linear self-interactions of the linear mode and have, therefore, the following form:

$$\begin{aligned} U_0(y,t) &= |\Phi(t)|^2 u_0^{(2)}(y)+|\Phi(t)|^4 u_0^{(4)}(y)+\cdots, \\ U_2(y,t) &= \Phi^2(t)u_2^{(2)}(y)+\Phi^2(t)|\Phi(t)|^2 u_2^{(4)}(y)+\cdots, \\ U_3(y,t) &= \Phi^3(t)u_3^{(3)}(y)+\cdots, \\ &\cdots \end{aligned} \tag{7}$$

where $u_0^{(2)}(y)$, $u_0^{(4)}(y)$ etc. are unknown functions. Substituting the ansatz (6) into eq.(4) and separating the terms proportional to $e^{i(k_x x+k_z z)}$ we obtain

$$\begin{aligned} \left(\frac{d\Phi}{dt}-\lambda\Phi\right)e^{i(k_x x+k_z z)}V_0(y) &= \bar{N}\left(\Phi e^{i(k_x x+k_z z)}V_0(y),U_0(y,t)\right) \\ &+\bar{N}\left(\Phi^* e^{-i(k_x x+k_z z)}V_0^*(y),e^{2i(k_x x+k_z z)}U_2(y,t)\right) \\ &+\sum_{n=2}^{\infty}\bar{N}\left(e^{(n+1)i(k_x x+k_z z)}U_{n+1}(y,t),e^{-ni(k_x x+k_z z)}U_n^*(y,t)\right), \end{aligned} \tag{8}$$

where $\bar{N}(A,B)=N(A,B)+N(B,A)$. The evolution equation for the amplitude Φ can be derived with the help of the eigenmode of the adjoint operator $\hat{\mathcal{L}}^\dagger$, which is defined via

$$\langle V_1|\hat{\mathcal{L}}V_2\rangle=\langle\hat{\mathcal{L}}^\dagger V_1|V_2\rangle, \tag{9}$$

where the scalar product is given by

$$\langle V_1|V_2\rangle=\lim_{L_x,L_z\to\infty}\frac{1}{2L_x}\int_{-L_x}^{L_x}dx\,\frac{1}{2}\int_{-1}^{1}dy\,\frac{1}{2L_z}\int_{-L_z}^{L_z}dz\;(V_1^*,V_2), \tag{10}$$

and $(A,B)=\sum_i A_i B_i$. The eigenmodes of the adjoint operator

$$\hat{\mathcal{L}}^{\dagger}\left(e^{i(k_x x+k_z z)}W_0^{(m)}(y)\right)=-\lambda_m e^{i(k_x x+k_z z)}W_0^{(m)}(y) \tag{11}$$

are orthogonal to the eigenfunctions of the linear operator $\hat{\mathcal{L}}$ unless their eigenvalues coincide $\lambda_n=\lambda_m$ (see eq.(5)). Using this property, we project eq.(8) onto the eigenfunction V_0 to obtain the amplitude equation

$$\frac{d\Phi}{dt}=\lambda\Phi+C_3\Phi|\Phi|^2+C_5\Phi|\Phi|^4+C_7\Phi|\Phi|^6+C_9\Phi|\Phi|^8+\cdots, \tag{12}$$

where the coefficients are given by

$$C_3=\frac{1}{\Delta}\Big\langle e^{i(k_x x+k_z z)}W_0(y)\Big|\bar{N}\left(e^{i(k_x x+k_z z)}V_0(y),u_0^{(2)}(y)\right) +\bar{N}\left(e^{-i(k_x x+k_z z)}V_0^*(y),e^{2i(k_x x+k_z z)}u_2^{(2)}(y)\right)\Big\rangle, \tag{13}$$

$$C_5=\frac{1}{\Delta}\Big\langle e^{i(k_x x+k_z z)}W_0(y)\Big|\bar{N}\left(e^{i(k_x x+k_z z)}V_0(y),u_0^{(4)}(y)\right) +\bar{N}\left(e^{-i(k_x x+k_z z)}V_0^*(y),e^{2i(k_x x+k_z z)}u_2^{(4)}(y)\right) +\bar{N}\left(e^{-2i(k_x x+k_z z)}u_2^{(2)*}(y),e^{3i(k_x x+k_z z)}u_3^{(3)}(y)\right)\Big\rangle, \tag{14}$$

...

with $\Delta=\langle e^{i(k_x x+k_z z)}W_0(y)|e^{i(k_x x+k_z z)}V_0(y)\rangle$. The expressions for higher coefficients C_7, C_9 etc. are derived in the similar way. The equations for the unknown functions $u_0^{(2)}(y)$, $u_0^{(4)}(y)$ etc. are also derived by substituting the ansatz (6) into eq.(4) and are given in Appendix B.

In this work we are going to calculate the first five coefficients C_3 – C_{11} of eq.(12) for plane Couette flow of a UCM fluid. In the next Section we present the results for various eigenfunctions and discuss their non-linear stability.

2. Results

Since our analysis is based on the eigenfunctions of the linear operator $\hat{\mathcal{L}}$, we first discuss the structure of the linear spectrum $\{\lambda_n\}$ for given Reynolds and Weissenberg numbers.

The eigenvalues of the UCM plane Couette flow problem can be separated in two groups: the "purely elastic" eigenvalues and "elastic-inertial" ones. The first group consists of a pair of complex conjugated eigenvalues and the so-called "continuous spectrum". The eigenvalues from this group are "purely

elastic" in the sense that they exist even in the limit $Re = 0$. The pair was discovered by Gorodtsov and Leonov (Gorodtsov and Leonov, 1967) for two-dimensional purely elastic plane Couette flow and can be generalized to the 3-dimensional case:

$$\lambda^{(GL)} = \epsilon \pm i\omega \tag{15}$$

$$\epsilon = \frac{1}{D}\left[k_x\, k\, q\, \sin\left(2\, Wi\, k_x\right) - \frac{1}{2}\, Wi\, k_x^2 \sinh\left(2\, k\right) \sinh\left(2\, q\right)\right]$$

$$\omega^2 = -\epsilon^2 + k_x^2 - \frac{k_x^2}{D}\Big[2\, k\, q\, \cos\left(2\, Wi\, k_x\right) + q\, \cosh\left(2\, q\right) \sinh\left(2\, k\right) - \frac{1}{2} \sinh\left(2\, q\right) \left(2\, k\, \cosh\left(2\, k\right) + \sinh\left(2\, k\right)\right)\Big],$$

where

$$k = \sqrt{k_x^2 + k_z^2}\ , \qquad q = \sqrt{(1 + Wi^2)k_x^2 + k_z^2},$$

$$D = k\, q\Big(\cos 2\, Wi\, k_x - \cosh\left(2\, k\right) \cosh\left(2\, q\right)\Big) + q^2\, \sinh\left(2\, k\right) \sinh\left(2\, q\right).$$

For small Reynolds numbers, the Gorodtsov-Leonov eigenvalues pick up corrections of order Re. This pair of eigenvalues corresponds to the 3-dimensional vortices localized at the walls and traveling along them in opposite directions. An example of the velocity field generated by such an eigenmode is plotted in Fig.1 for $\lambda^{(GL)} = -0.9273 + 0.7279i$, $Wi = 1$, $Re = 0.1$, $k_x = 1$ and $k_z = 1$.

The continuous spectrum contains infinitely many eigenvalues in the form (Renardy and Renardy, 1986, Wilson et al., 1999)

$$\lambda^{(C)} = -\frac{1}{Wi} + i\,\omega\ , \qquad \omega \in [-k_x, k_x]. \tag{16}$$

and, as was shown by Graham (Graham, 1998), is unphysical. It has its origin in the fact that polymers with non-linear relation between the degree of extension and the force necessary to achieve this extension behave as Hookean dumbbells upon linearization, while the latter can be infinitely stretched in extensional flow at finite Weissenberg numbers (Bird et al., 1987). Indeed, Graham has found (Graham, 1998) that the stresses of the eigenmodes corresponding to $\lambda^{(C)}$ have singularities and are unrealistic. These eigenvalues will be discarded in our work.

The second group contains infinitely many eigenvalues that disappear in the limit of $Re \to 0$. The eigenvalues from this group have their real parts close to $1/2Wi$, while their imaginary parts scale as $1/\sqrt{Re}$; they can be ordered according to an integer n that gives the number of wiggles in the y-direction. The "elastic-inertial" eigenvalues can further be split in two infinite subsets,

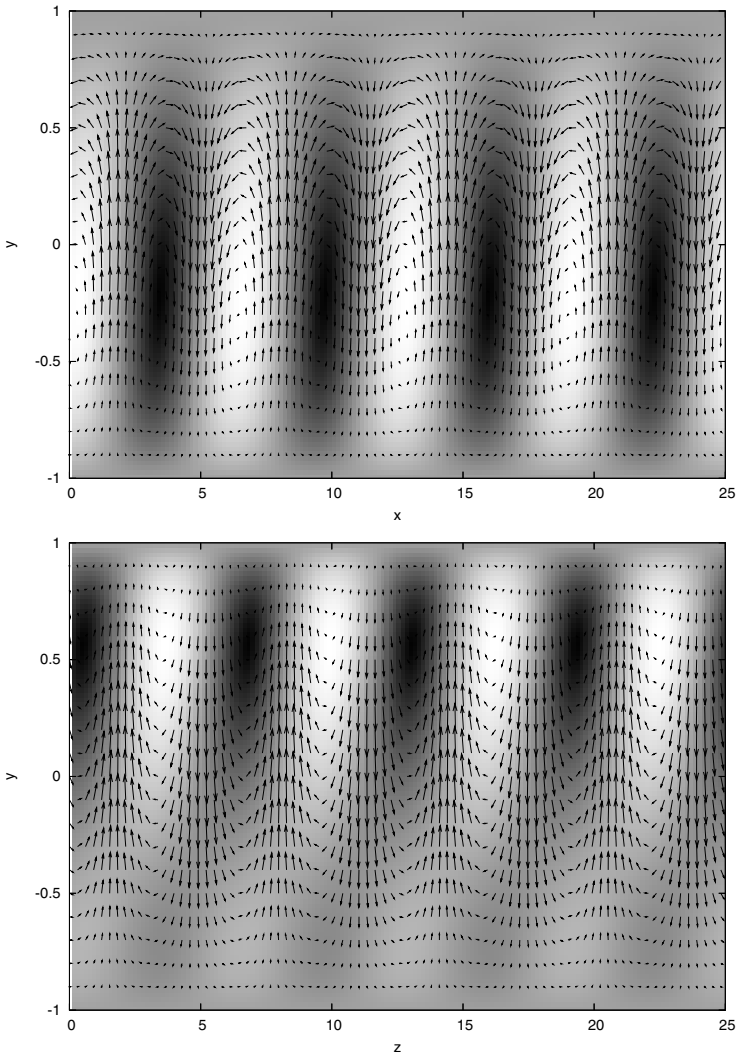

Figure 1. Velocity field of the Gorodtsov-Leonov eigenmode with $\lambda^{(GL)} = -0.9273 + 0.7279i$, $Wi = 1$, $Re = 0.1$, $k_x = 1$ and $k_z = 1$. The eigenmode is mostly localized near one wall, while the eigenmode with the complex-conjugated eigenvalue $\lambda^{(GL)} = -0.9273 - 0.7279i$ occupies the other. *Top:* velocity field in the xy-plane. The shade of gray represents the third velocity component; *Middle:* The same in the yz-plane.

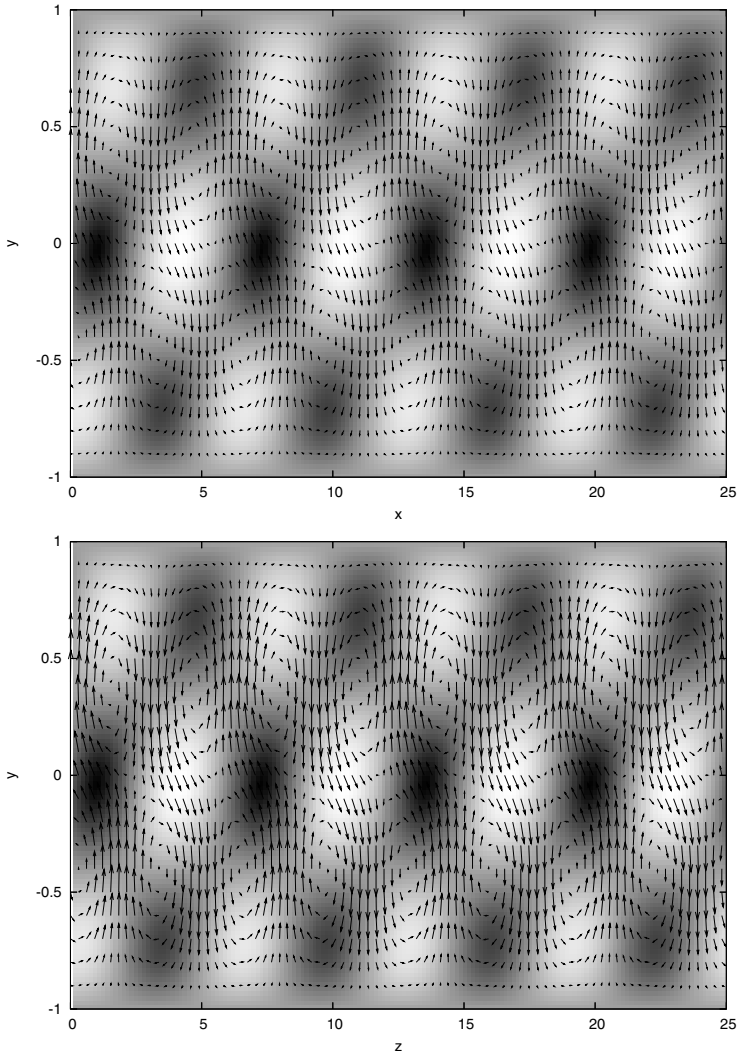

Figure 2. Velocity field of the "elastic-inertial" eigenmode with $\lambda = -0.4924 + 14.9384i$, $Wi = 1$, $Re = 0.1$, $k_x = 1$ and $k_z = 1$. *Top:* velocity field in the xy-plane. The shade of gray represents the third velocity component; *Bottom:* The same in the yz-plane.

corresponding to 2- and 3-dimensional vortices. An example of the 3D vortices is given in Fig.2. The difference between the structure of the 2D and 3D vortices becomes apparent if $k_x = 0$: they reduce to the streamwise streaks and a combination of the streamwise streaks and vortices, respectively.

All of the eigenvalues discussed have negative real parts and are, therefore, linearly stable.

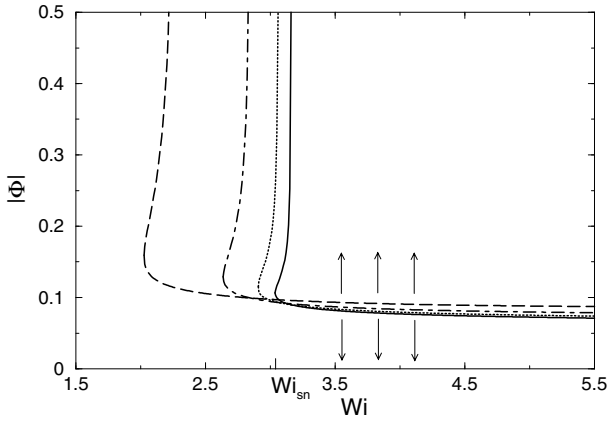

Figure 3. Steady-state amplitude Φ for $k_x = 1$ and $k_z = 1$ versus Weissenberg number Wi. The curves from left to right represent the solutions to $S_2 = 0, \cdots, S_5 = 0$, respectively. The ratio $Re = 10^{-3} Wi$ was kept constant.

Now we turn to the non-linear stability analysis of the eigenmodes discussed above. For each eigenvalue λ we calculate the coefficients C's in eq.(12) with the help of eqs.(13,14,11) and the equations from Appendix B. This calculation requires solution of several linear inhomogeneous ODE's of the 4th order. For the special case of the inertialess ($Re = 0$) Gorodtsov-Leonov eigenmode we were able to calculate the coefficients C_3 and C_5 analytically. The higher coefficients and the coefficients for the other eigenmodes involve long and cumbersome expressions and were treated numerically. Since the ODE's from Appendix B are very stiff, we solved them using the 4th-order Runge-Kutta method with reortonormalization performed at each step (Godunov, 1961, Conte, 1966). Our code was tested against the analytical result for the inertialess Gorodtsov-Leonov eigenmode.

The instability threshold $|\Phi_*|$ is given by the amplitude of the traveling-wave solution, $\Phi(t) = |\Phi_*|\, e^{i\,\Omega\, t}$, of eq.(12)

$$S_m(|\Phi_*|) \equiv Re\left(\lambda + C_3|\Phi_*|^2 + \cdots + C_{2m+1}|\Phi_*|^{2m}\right) = 0. \qquad (17)$$

However, one has to be careful because it is not guaranteed that the asymptotic series (17) converges. Thus, the amplitude expansion for the Newtonian channel flow was shown to suffer from convergence problems (Herbert, 1980). Therefore, we solve the sequence of equations $S_2 = 0, \cdots, S_5 = 0$ in order to check that their solutions do converge to some value $|\Phi_*|$.

The results for the Gorodtsov-Leonov eigenmodes are shown in Figs.3 and 4. The most important feature of these curves is that they show the existence of a subcritical instability for Weissenberg numbers larger than the saddle-node value $Wi_{\rm sn}$. As the arrows indicate, for $Wi > Wi_{\rm sn}$ the lower branch

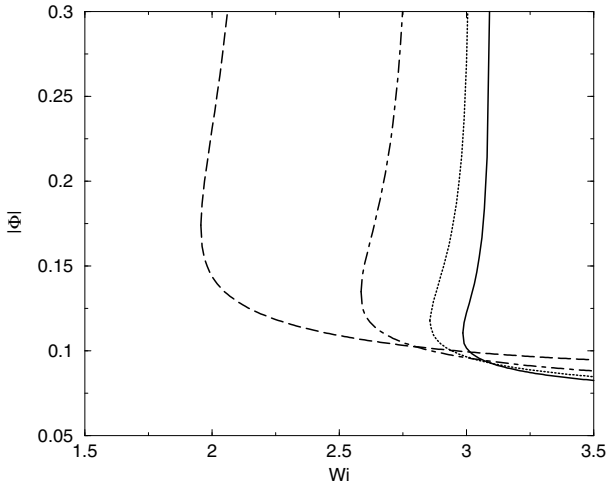

Figure 4. The same as Fig.3 for $k_x = 2$, $k_z = 2$, and $Re = 10^{-1}Wi$.

of the curves denotes the critical amplitude – amplitudes larger than this value will grow in time. Note that the instability threshold is small (consistent with the assumption $|\Phi| < 1$), and goes down as Wi increases. The inclusion of higher-order terms causes the whole curve to shift to the right, though the shift becomes roughly two times smaller with every coefficient included, suggesting convergence.

Table 1. Real parts of the coefficients C's for $k_x = 2$, $k_z = 2$, and $Re = 10^{-1}Wi$; ϵ and ω denote the real and imaginary parts of the Gorodtsov-Leonov eigenvalue, respectively.

Wi	ϵ	ω	C_3	$C_5 \times 10^{-2}$	$C_7 \times 10^{-5}$	$C_9 \times 10^{-7}$	$C_{11} \times 10^{-9}$
1.50	0.562	1.757	39.549	-21.322	-5.723	-7.617	-5.683
2.00	0.394	1.796	26.433	-3.571	-2.020	-3.169	-3.162
2.20	0.350	1.809	23.802	-0.011	-1.308	-2.344	-2.741
2.30	0.331	1.815	22.720	1.376	-1.019	-1.986	-2.495
2.80	0.259	1.841	18.642	5.740	-0.001	-0.517	-0.972
2.90	0.248	1.845	18.000	6.249	0.141	-0.276	-0.641
3.00	0.238	1.849	17.399	6.672	0.267	-0.053	-0.312
3.05	0.233	1.851	17.112	6.855	0.324	0.053	-0.149
3.10	0.228	1.853	16.833	7.021	0.378	0.155	0.012
5.50	0.113	1.912	9.096	6.926	1.112	2.243	4.802

While the lower branch of each curves gives the minimal amplitude of the disturbance sufficient to destabilize the laminar flow, the upper branch determines the saturated value of Φ after the transition. Surprisingly, it diverges

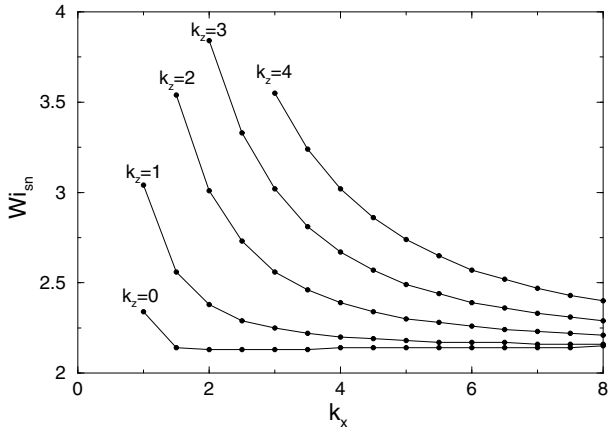

Figure 5. The saddle-node Weissenberg number versus k_x for different values of k_z; $Re = 10^{-3}Wi$.

in the vicinity of the saddle-node where the highest coefficient in the expansion changes sign (see Table 1). There could be several reasons for that. First, it may indicate that the non-linear state in the form of eq.(6) is unstable and will undergo a transition to another coherent state or to turbulence. Second, although we consider this unlikely, it may be that the UCM model cannot capture this state. Finally, and most likely, it may be that the upper branch lies beyond the radius of convergence of (12).

In Fig.5 we plot the lowest Weissenberg number for which the non-linear instability is possible, or the position of the saddle-node $Wi_{\rm sn}$, as a function of the wave-vectors k_x and k_z. It clearly shows that the saddle-node position is only a weak function of the wave-vectors, and a large number of modes with different k_x's and k_z's is non-linearly unstable for given $Wi > 2.1$. Even if each individual mode saturates at a given value of Φ, we cannot predict the behaviour of the superposition of a large number of such modes. They might stabilize each other to form a 3-dimensional coherent state, or they can become chaotic very close to or even at the instability.

Finally, we turn to the discussion of the "elastic-inertial" eigenmodes. We have performed calculations for the first ten of these modes and have found that for all of them the real parts of the coefficients C's are negative. Hence, we do not find a subcritical instability if the perturbation is chosen in the form of the "elastic-inertial" eigenmodes. An interesting question is whether these eigenmodes contribute to the visco-elastic exact coherent state (if such a state exists !), or whether this state is a non-linear superposition of the Gorodtsov-Leonov eigenmodes only. To this moment, it remains an open question.

3. Discussion

We have presented the non-linear stability analysis of the visco-elastic plane Couette flow of the UCM model. We have derived the amplitude equation describing the time-evolution of a perturbation chosen in the form of an eigenmode of the linear operator, and have shown that for the purely elastic Gorodtsov-Leonov eigenmodes, there exists a subcritical instability for the Weissenberg numbers $Wi > 2.1$. The other eigenmodes are found to be non-linearly stable.

As Fig.5 shows, the saddle-node Weissenberg number is a weak function of the wave-vectors k_x and k_z and an infinite number of the Gorodtsov-Leonov eigenmodes will become unstable for $Wi > 2.1$. The nature of the state that will result from the non-linear interactions of these modes is unknown. The possibilities include a turbulent state, a stable 3D coherent state and a linearly unstable 3D coherent state, in which case it will be a visco-elastic analog of the Newtonian Nagata solutions (Nagata, 1990). If such a state exists and is linearly unstable, there is an intriguing possibility that it will take part in the visco-elastic version of the self-sustaining cycle proposed by Waleffe (Waleffe, 1997).

The previous studies of the visco-elastic plane Couette flow were inconclusive but might well be taken to be in agreement with our findings though they also were not able to capture the non-linear state after the instability. Atalik and Keunings (Atalik and Keunings, 2002) performed 2D direct numerical simulations of the Oldroyd-B plane Couette flow, and have shown that it is stable for Weissenberg numbers smaller than 2. Moreover, they reported appearance of numerical instabilities for Weissenberg numbers larger than 2. It is tempting to speculate that the numerical instability observed by Atalik and Keunings is a manifestation of the underlying physical instability. Ashrafi and Khayat (Ashrafi and Khayat, 2000) have developed a low-dimensional Galerkin projection for the Johnson-Segalman fluid, and have shown that one-dimensional disturbances in x-direction become unstable. There as well, one cannot draw a conclusion about the resulting state in view of the special form of the perturbation and the very small number of modes included.

Finally, we want to make a general comment on the application of the amplitude expansion to the non-linear stability analysis of the visco-elastic flows. Surely, this method is crude for it a) ignores interactions between various eigenmodes, b) assumes "slaving" (see Section 1 for details), c) requires amplitude of the perturbation to be small etc. It is incomparable in conclusiveness and accuracy with the modern methods used in Newtonian instabilities. These methods, however, are difficult to employ for the visco-elastic instabilities as they rely heavily on the insights from numerical and experimental studies. Let us repeat that there has been no experimental or numerical study of the visco-elastic parallel shear flows. The low-dimensional models are also

difficult to derive in the visco-elastic case, as we simply do not know what kind of coherent structures may get involved. Experiments in Taylor-Couette flow of Groisman and Steinberg (Groisman and Steinberg, 1997) and numerical study of Kumar and Graham (Kumar and Graham, 2000) suggest that the coherent structures in visco-elastic plane Couette flow may be different from the Newtonian counterparts. Therefore, the present study is a first step towards understanding visco-elastic instabilities in parallel shear flows.

Acknowledgments

The work by ANM is financially supported by the Dutch physics funding foundation FOM.

Appendix

As we have mentioned above, the equations of motion (1)-(3) can be written in the matrix form

$$\hat{\mathcal{L}}\, V + \hat{A}\frac{\partial V}{\partial t} = N\left(V, V\right),$$

where $\hat{A}$ is a constant matrix

$$A_{ij} = \begin{cases} 0 & i \neq j \\ Re & i = j = 1 \ldots 3 \\ 0 & i = j = 4 \\ Wi & i = j = 5 \ldots 10 \end{cases}$$

and $\hat{\mathcal{L}}$ is the linear operator

$$\hat{\mathcal{L}} = \begin{pmatrix} \hat{K} & Re & 0 & \partial_x & \partial_y & \partial_z & 0 & 0 & 0 & \partial_x \\ 0 & \hat{K} & 0 & 0 & \partial_x & 0 & \partial_y & \partial_z & 0 & \partial_y \\ 0 & 0 & \hat{K} & 0 & 0 & \partial_x & 0 & \partial_y & \partial_z & \partial_z \\ \partial_x & \partial_y & \partial_z & 0 & 0 & 0 & 0 & 0 & 0 & 0 \\ 2\hat{X}_1 & 0 & 0 & \hat{L} & -2\,Wi & 0 & 0 & 0 & 0 & 0 \\ \partial_y & (1+2\,Wi^2)\,\partial_x & -Wi\,\partial_z & 0 & \hat{L} & 0 & -Wi & 0 & 0 & 0 \\ \partial_z & 0 & \hat{X}_1 & 0 & 0 & \hat{L} & 0 & -Wi & 0 & 0 \\ 0 & 2\hat{X}_2 & 0 & 0 & 0 & 0 & \hat{L} & 0 & 0 & 0 \\ 0 & \partial_z & \hat{X}_2 & 0 & 0 & 0 & 0 & \hat{L} & 0 & 0 \\ 0 & 0 & 2\,\partial_z & 0 & 0 & 0 & 0 & 0 & \hat{L} & 0 \end{pmatrix},$$

where $\hat{L} = 1 + Wi\, y\, \partial_x$, $\hat{K} = Re\, y\, \partial_x$, $\hat{X}_1 = (1+2\,Wi^2)\,\partial_x + Wi\,\partial_y$, and $\hat{X}_2 = Wi\,\partial_x + \partial_y$.

The bilinear form N represent the non-linear terms in eqs.(1)-(3)

$$N\left(V^{(A)}, V^{(B)}\right) = -\left(\mathbf{v}^{(A)} \cdot \nabla\right) \hat{A} \cdot V^{(B)}$$

$$+Wi \begin{pmatrix} 0 \\ 0 \\ 0 \\ 0 \\ 2\left[\tau_{xx}^{(A)}\partial_x v_x^{(B)} + \tau_{xy}^{(A)}\partial_y v_x^{(B)} + \tau_{xz}^{(A)}\partial_z v_x^{(B)}\right] \\ \tau_{xx}^{(A)}\partial_x v_y^{(B)} - \tau_{xy}^{(A)}\partial_z v_z^{(B)} + \tau_{xz}^{(A)}\partial_z v_y^{(B)} + \tau_{yy}^{(A)}\partial_y v_x^{(B)} + \tau_{yz}^{(A)}\partial_z v_x^{(B)} \\ \tau_{xx}^{(A)}\partial_x v_z^{(B)} + \tau_{xy}^{(A)}\partial_y v_z^{(B)} - \tau_{xz}^{(A)}\partial_y v_y^{(B)} + \tau_{yz}^{(A)}\partial_y v_x^{(B)} + \tau_{zz}^{(A)}\partial_z v_x^{(B)} \\ 2\left[\tau_{xy}^{(A)}\partial_x v_y^{(B)} + \tau_{yy}^{(A)}\partial_y v_y^{(B)} + \tau_{yz}^{(A)}\partial_z v_y^{(B)}\right] \\ \tau_{xy}^{(A)}\partial_x v_z^{(B)} + \tau_{xz}^{(A)}\partial_x v_y^{(B)} + \tau_{yy}^{(A)}\partial_y v_z^{(B)} - \tau_{yz}^{(A)}\partial_x v_x^{(B)} + \tau_{zz}^{(A)}\partial_z v_y^{(B)} \\ 2\left[\tau_{xz}^{(A)}\partial_x v_z^{(B)} + \tau_{yz}^{(A)}\partial_y v_z^{(B)} + \tau_{zz}^{(A)}\partial_z v_z^{(B)}\right] \end{pmatrix}$$

Obviously, $N\left(A, B\right) \neq N\left(B, A\right)$.

Appendix B

The equations for the unknown functions $u_0^{(2)}(y)$, $u_0^{(4)}(y)$ etc. are derived by substituting the ansatz (6) into eq.(4). Requiring that the coefficients of the harmonics $e^{in(k_x x+k_z z)}$ vanish for all n's one obtains

$$\hat{\mathcal{L}}\left(e^{2i\xi}u_2^{(2)}\right) + 2\lambda e^{2i\xi}u_2^{(2)} = N\left(e^{i\xi}V_0, e^{i\xi}V_0\right)$$

$$\hat{\mathcal{L}}\left(e^{2i\xi}u_2^{(4)}\right) + 2\left(\lambda + \Re\lambda\right)e^{2i\xi}u_2^{(4)} = -2C_3 e^{2i\xi}u_2^{(2)} + \bar{N}\left(e^{-i\xi}V_0^*, e^{3i\xi}u_3^{(3)}\right) + \bar{N}\left(u_0^{(2)}, e^{2i\xi}u_2^{(2)}\right)$$

$$\hat{\mathcal{L}}\left(u_0^{(2)}\right) + 2\left(\Re\lambda\right)u_0^{(2)} = \bar{N}\left(e^{i\xi}V_0, e^{-i\xi}V_0^*\right)$$

$$\hat{\mathcal{L}}\left(u_0^{(4)}\right) + 4\left(\Re\lambda\right)u_0^{(4)} = -2\left(\Re C_3\right)u_0^{(2)} + N\left(u_0^{(2)}, u_0^{(2)}\right) + \bar{N}\left(e^{2i\xi}u_2^{(2)}, e^{-2i\xi}u_2^{(2)*}\right)$$

$$\hat{\mathcal{L}}\left(e^{3i\xi}u_3^{(3)}\right) + 3\lambda e^{3i\xi}u_3^{(3)} = \bar{N}\left(e^{i\xi}V_0, e^{2i\xi}u_2^{(2)}\right)$$

where $\xi = k_x x + k_z z$ and $\Re$ denotes the real part of a complex number. In deriving these equations one has to deal with the expressions like $\frac{\partial U_n(y,t)}{\partial t}$ or, in view of eq.(7), with $\frac{d\Phi(t)}{dt}$. This derivative is replaced by the r.h.s. of the amplitude equation (12) to assure self-consistency.

References

Ashrafi, N. and Khayat, R. E. (2000). A low-dimensional approach to nonlinear plane-Couette flow of viscoelastic fluids. *Phys. Fluids*, 12:345–365.

Atalik, K. and Keunings, R. (2002). Non-linear temporal stability analysis of viscoelastic plane channel flows using a fully-spectral method. *J. Non-Newtonian Fluid Mech.*, 102:299–319.

Bertola, V., Meulenbroek, B., Wagner, C., Storm, C., Morozov, A. N., van Saarloos, W., and Bonn, D. (2003). Experimental evidence for an intrinsic route to polymer melt fracture phenomena: A nonlinear instability of viscoelastic Poiseuille flow. *Phys. Rev. Lett.*, 90:114502.

Bird, R. B., Armstrong, R. C., and Hassager, O. (1987). *Dynamics of polymeric liquids*, volume 1. John Wiley & Sons, Inc., 2nd edition.

Conte, S. D. (1966). The numerical solution of linear boundary value problems. *SIAM Review*, 8:309–321.

Denn, M. M. (1990). Issues in visco-elastic fluid-mechanics. *Annu. Rev. Fluid Mech.*, 22:13–34.

Denn, M. M. (2001). Extrusion instabilities and wall slip. *Annu. Rev. Fluid Mech.*, 33:265–287.

Godunov, S. (1961). On the numerical solution of boundary value problems for systems of linear ordinary differential equations. *Uspehi Mat. Nauk*, 16:171–174.

Gorodtsov, V. A. and Leonov, A. I. (1967). On a linear instability of a parallel Couette flow of viscoelastic fluid. *J. Appl. Math. Mech.*, 31:310–319.

Graham, M. D. (1998). Effect of axial flow on viscoelastic Taylor-Couette instability. *J. Fluid Mech.*, 360:341–374.

Grillet, A. M., Bogaerds, A. C. B., Peters, G. W. M., and Baaijens, F. P. T. (2002). Stability analysis of constitutive equations for polymer melts in viscometric flows. *J. Non-Newtonian Fluid Mech.*, 103:221–250.

Groisman, A. and Steinberg, V. (1997). Solitary vortex pairs in viscoelastic Couette flow. *Phys. Rev. Lett.*, 78:1460–1463.

Groisman, A. and Steinberg, V. (2000). Elastic turbulence in a polymer solution flow. *Nature*, 405:53.

Groisman, A. and Steinberg, V. (2004). Elastic turbulence in curvilinear flows of polymer solutions. *New J. Phys.*, 6:29.

Herbert, T. (1980). Nonlinear stability of parallel flows by high-order amplitude expansions. *AIAA Journal*, 18:243–248.

Ho, T. C. and Denn, M. M. (1977/1978). Stability of plane Poiseuille flow of a highly elastic liquid. *J. Non-Newtonian Fluid Mech.*, 3:179–195.

Hof, B., Juel, A., and Mullin, T. (2003). Scaling of the turbulence transition threshold in a pipe. *Phys. Rev. Lett.*, 91:244502.

Joo, Y. L. and Shaqfeh, E. S. G. (1992). A purely elastic instability in Dean and Taylor-Dean flow. *Phys. Fluids A*, 4:524.

Kumar, K. A. and Graham, M. (2000). Solitary coherent structures in viscoelastic shear flow: Computation and mechanism. *Phys. Rev. Lett.*, 85:4056.

Larson, R. (2000). Turbulence without inertia. *Nature*, 405:27.

Larson, R. G., Shaqfeh, E. S. G., and Muller, S. J. (1990). A purely elastic instability in Taylor-Couette flow. *J. Fluid Mech.*, 218:573–600.

McKinley, G. H., Byars, J. A., Brown, R. A., and Armstrong, R. C. (1991). Observations on the elastic instability in cone-and-plate and parallel plate flows of a polyisobutylene Boger fluid. *J. Non-Newtonian Fluid Mech.*, 40:201–229.

Meulenbroek, B., Storm, C., Bertola, V., Wagner, C., Bonn, D., and van Saarloos, W. (2003). Intrinsic route to melt fracture in polymer extrusion: A weakly nonlinear subcritical instability of viscoelastic Poiseuille flow. *Phys. Rev. Lett.*, 90:024502.

Meulenbroek, B., Storm, C., Morozov, A. N., and van Saarloos, W. (2004). Weakly nonlinear subcritical instability of visco-elastic Poiseuille flow. *J. Non-Newtonian Fluid Mech.*, 116:235–268.

Nagata, M. (1990). Three-dimensional finite-amplitude solutions in plane Couette flow: bifurcation from infinity. *J. Fluid Mech.*, 217:519–527.

Owens, R. G. and Phillips, T. N. (2002). *Computational Rheology*. Imperial College Press.

Pakdel, P. and McKinley, G. H. (1996). Elastic instability and curved streamlines. *Phys. Rev. Lett.*, 77:2459.

Petrie, C. J. S. and Denn, M. M. (1976). Instabilities in polymer processing. *AICHE J.*, 22:209–236.

Renardy, M. (1992). A rigorous stability proof for plane Couette flow of an upper convected Maxwell fluid at zero Reynolds number. *Eur. J. Mech. B*, 11:511–516.

Renardy, M. and Renardy, Y. (1986). Linear stability of plane Couette flow of an upper convected Maxwell fluid. *J. Non-Newtonian Fluid Mech.*, 22:23–33.

Schmid, P. J. and Henningson, D. S. (2001). *Stability and transition in shear flows*. Springer-Verlag, New York.

Stuart, J. T. (1960). On the non-linear mechanics of wave disturbances in stable and unstable parallel flows. *J. Fluid Mech.*, 9:353–370.

Waleffe, F. (1997). On a self-sustaining process in shear flows. *Phys. Fluids*, 9:883–900.

Wilson, H. J., Renardy, M., and Renardy, Y. (1999). Structure of the spectrum in zero Reynolds number shear flow of the UCM and Oldroyd-B liquids. *J. Non-Newtonian Fluid Mech.*, 80:251–268.